SARS-CoV-2 vaccination can elicit a CD8 T-cell dominant hepatitis

Tobias Boettler [1], *, Benedikt Csernalabics [1], *, Henrike Salié [1], Hendrik Luxenburger [1], Lara Wischer [1], Elahe Salimi Alizei [1,2], Katharina Zoldan [1], Laurenz Krimmel [1], Peter Bronsert [3], Marius Schwabenland [4], Marco Prinz [4,5], Carolin Mogler [6], Christoph Neumann-Haefelin [1], Robert Thimme [1], Maike Hofmann [1], *, Bertram Bengsch [1,5,7] ⧄ * ✉

Show more ⌄

≔ Outline   ⊶ Share   ❞ Cite

Get rights and content

Highlights

- Identification of immune correlates in a case of mRNA vaccine-associated autoimmune hepatitis

- Imaging mass cytometry identifies intrahepatic panlobular enrichment of activated cytotoxic CD8 T cells

- Flow cytometry identifies intrahepatic enrichment of activated CD8 T cells with SARS-CoV-2-specificity

- Peripheral SARS-CoV-2-specific CD8 T cell activation correlates with ALT levels

Abstract

Background & Aims

Autoimmune hepatitis episodes have been described following SARS-CoV-2 infection and vaccination but their pathophysiology remains unclear. Here, we report the case of a 52-year-old male, presenting with bimodal episodes of acute hepatitis, each occurring 2-3 weeks after BNT162b2 mRNA vaccination and sought to identify the underlying immune correlates. The patient received first oral budesonide, relapsed, but achieved remission under systemic steroids.

Methods

Imaging mass cytometry for spatial immune profiling was performed on liver biopsy tissue. Flow cytometry was performed to dissect CD8 T cell phenotypes and identify SARS-CoV-2-specific and EBV-specific T cells longitudinally. Vaccine-induced antibodies were determined by ELISA. Data was correlated with clinical labs.

Results

Analysis of the hepatic tissue revealed an immune infiltrate quantitatively dominated by activated cytotoxic CD8 T cells with panlobular distribution. An enrichment of CD4 T cells, B cells, plasma cells and myeloid cells was also observed compared to controls. The intrahepatic infiltrate showed enrichment for CD8 T cells with SARS-CoV-2-specificity compared to the peripheral blood. Notably, hepatitis severity correlated longitudinally with an activated cytotoxic phenotype of peripheral SARS-CoV-2-specific, but not EBV-specific CD8+ T cells or vaccine-induced immunoglobulins.

Conclusions

COVID19 vaccination can elicit a distinct T cell-dominant immune-mediated hepatitis with a unique pathomechanism associated with vaccination induced antigen-specific tissue-resident immunity requiring systemic immunosuppression.

Lay summary

Liver inflammation is observed during SARS-CoV-2 infection but can also occur in some individuals after vaccination and shares some typical features with autoimmune liver disease. In this report, we show that highly activated T cells accumulate and are evenly distributed in the different areas of the liver in a patient with liver inflammation following SARS-CoV-2 vaccination. Moreover, within these liver infiltrating T cells, we observed an enrichment of T cells that are reactive to SARS-CoV-2, suggesting that these vaccine-induced cells can contribute to the liver inflammation in this context.

Graphical abstract
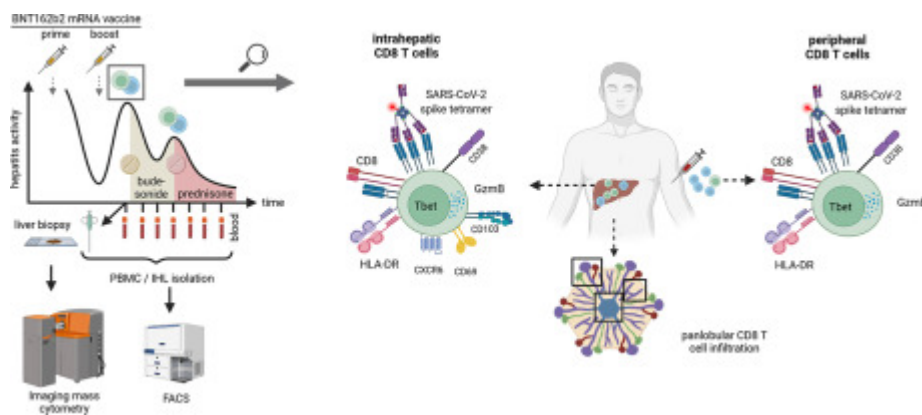
Keywords

COVID-19; vaccination; Autoimmune hepatitis; virus-specific T cell; CD8+ T cell; Immunosuppression

Introduction

Vaccination is the key strategy to fight the global COVID19 pandemic. There was no hepatitis safety signal in COVID19 vaccination trials[1], however several reports have recently associated autoimmune hepatitis (AIH)-like conditions with COVID19 vaccines[[2], [3], [4], [5], [6], [7], [8], [9], [10], [11]]. To our knowledge, no severe case with liver failure requiring liver transplantation was reported. Liver injury was observed after both, mRNA and vector-based vaccines, while time from vaccine administration to symptom onset ranged between 4 days after the first dose to 6 weeks after the second dose. One patient was re-exposed to the vaccine which led to a worsening of liver injury[11]. It remains unclear whether the reported association of autoimmune hepatitis with vaccination is coincidental, might reflect transient drug-induced liver injury, or could involve unique SARS-CoV-2-induced antigen-specific immune activation[12]. However, the fact that AIH-like conditions also occurred after SARS-CoV-2 infection[13] suggests that the latter could be a driving factor for the sporadic cases.

Here, we describe the case of a 52-year-old male presenting with acute mixed hepatocellular/cholestatic hepatitis after the first dose of BNT162b2 mRNA vaccine and severe hepatitis after the second dose. Diagnostic evaluation was compatible with criteria for autoimmune hepatitis (AIH). After initiation of oral budesonide therapy, liver function tests improved for a month before a relapse occurred that was successfully treated with systemic prednisolone and ursodeoxycholic acid. Comprehensive immunologic assessment of the inflammatory infiltrates in the liver revealed the presence of a highly activated cytotoxic CD8 T

cell infiltrate including a SARS-CoV-2-specific CD8 T cell population that correlated with the peripheral activation of SARS-CoV-2-specific CD8 T cells, indicating that post-COVID19 vaccination hepatitis involves vaccination-elicited antigen-specific immune responses with distinct histological features compared to bona fide autoimmune hepatitis.

Clinical course

The 52-year-old male patient with no remarkable medical history other than pre-existing hypothyroidism under long-term substitution therapy with levothyroxine and normal historic liver function tests (LFT) developed progressive nausea, fatigue, loss of appetite and pruritus with symptoms starting approximately 10 days after the first (prime) dose of the BNT162b2 mRNA vaccine. He subsequently developed jaundice and presented at his primary care physician with LFT indicative of acute mixed hepatocellular/cholestatic hepatitis (ALT: 2130 U/l, AP: 142 U/l gamma-GT: 217 U/l, Bilirubin 7.7 mg/dl) (Fig. 1). The patient was admitted to a primary care center 25 days post first vaccination. Viral hepatitis A, B, C and E as well as cytomegalovirus- and Epstein-Barr virus-infections were excluded by serology and/or PCR testing. HFE genotyping did not reveal hemochromatosis associated variations. There was also no significant alcohol consumption and autoimmune serology remained inconclusive with borderline AMA-M2 reactivity. The patient recovered rapidly without specific therapy and was discharged with decreasing LFTs after three days under leading differential diagnosis of a toxic hepatitis. Over the next two weeks, liver enzymes declined further, with normalization of AST and AP and the patient received his second (boost) dose of the BNT162b2 mRNA vaccine 41 days after the first vaccination (Fig. 1). 20 days post boost vaccination (dpb), the patient re-experienced nausea and fatigue. Lab testing revealed a relapse of acute mixed hepatitis with (ALT 1939 U/l, ALP 167 U/l, bilirubin 2.9 mg/dl). He was subsequently referred to our tertiary center at 26dpb. Autoimmune serology was repeated with mild Hyperglobulinemia (IgG levels 1.02-fold of ULN, normal IgA and IgM levels), ANA (1:200) and borderline positivity for anti-smooth muscle antibodies and AMA-M2 while tests for anti-LKM remained negative. We performed a liver biopsy that histologically showed interface hepatitis with a moderate degree of lymphoplasmacytic infiltrate and foci of lobular necrosis and apoptosis. Eosinophilic granulocytes were not present. Neither relevant perisinusoidal nor portal fibrosis were observed. Together, these findings are compatible with a probable autoimmune hepatitis according to the revised original score for autoimmune hepatitis[14] and the patient was treated with 9 mg oral budesonide per day. Over the next weeks liver enzymes declined before a relapse occurred 39 days after initiation of therapy (66 dpb), that was controlled subsequently after therapy escalation to systemic steroids in combination with ursodeoxycholic acid. The patient's LFTs subsequently normalized within 8 weeks (Fig. 1). Anti-spike antibodies did not show major fluctuations with similar titers compared to healthy individuals at the time of diagnosis at 27 days post boost vaccination (Fig. 1B) and an expected reduction of titers over time (Fig 1C).
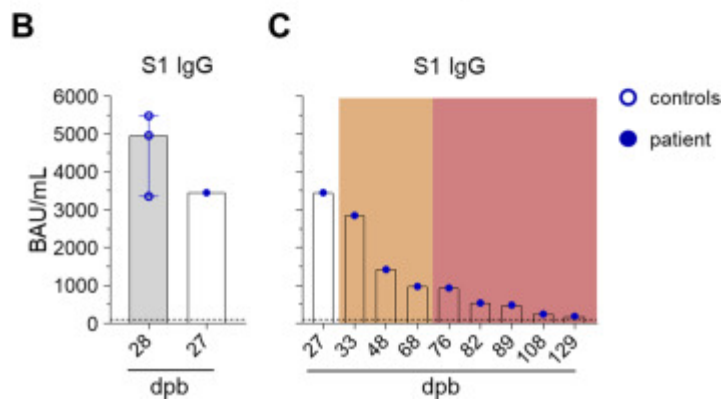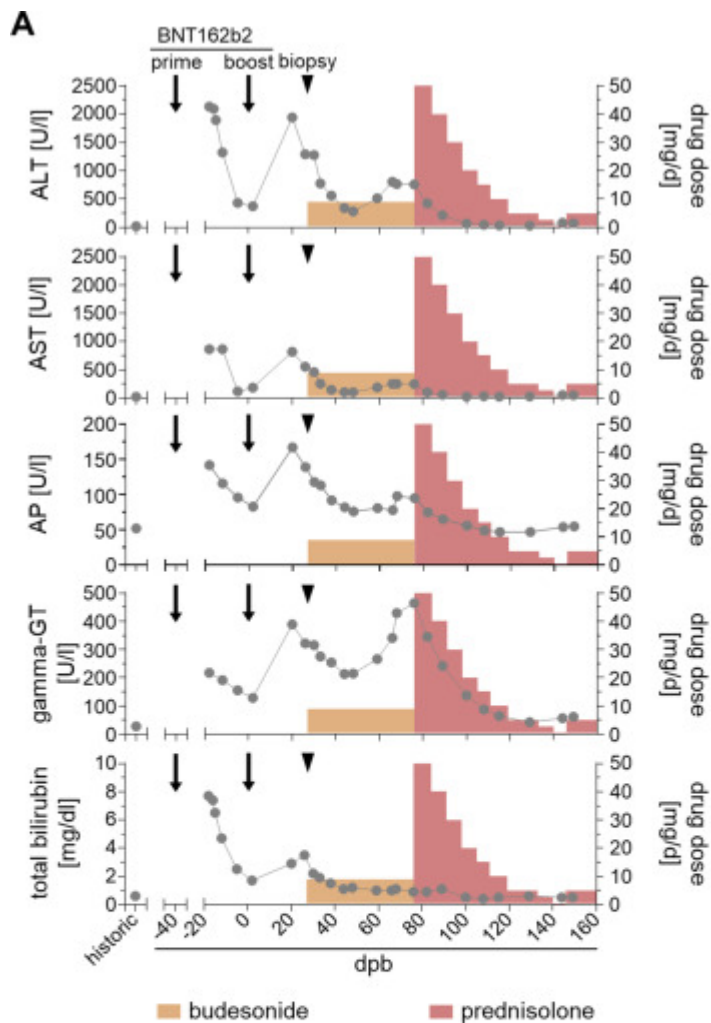
Figure 1. Clinical course with hepatitis after BNT162b2 vaccination. A: Time course of ALT, AST, ALP, gamma-GT and bilirubin levels after BNT162b2 vaccination in the patient. Arrows indicate the timepoint of BNT162b2 prime and boost vaccination. Arrowheads indicate timepoint of liver biopsy. Duration and dose of budesonide (9 mg/d) and prednisolone therapy (initially 50 mg/d) is shown in orange and red colorization. B: Comparison of anti-spike S1 IgG antibody titers in the patient to timepoint-matched vaccines who did not develop hepatitis. C: Longitudinal analysis of anti-spike S1 IgG antibodies before and after the initiation of therapy.

Results

Deep spatial immune analysis of liver tissue

To understand the immune infiltrate in the liver in more detail, in addition to conventional histochemistry, we performed highly multiplexed imaging mass cytometry with a broad panel covering relevant immune populations. As shown in figure 2A, this revealed infiltrates consisting of T cells, macrophages, B cells, plasma cells and granulocytes in the liver. The absolute number of immune cells was 5.3-fold increased compared to non-diseased control liver tissue obtained from liver resections (Fig. 2B). Interestingly, among the immune infiltrate, CD8 T cells represented the most abundant immune cell subset (465 per mm^2), which was unexpected for AIH. In contrast, B cells and plasma cells that are typically enriched in AIH, were found at relatively low numbers (102 per mm^2 and 66 per mm^2 respectively), even though these populations were also enriched in the immune infiltrate compared to controls (Fig. 2E). These findings suggested a different immune cell contribution compared to typical spontaneous AIH. We next assessed the spatial localization of the different immune cell subsets within the liver parenchyma. The strongest immune infiltration was observed in periportal areas (Fig. 2C). Notably, while B cells and plasma cells were also enriched but predominantly present in periportal areas, CD8 T cell distribution was panlobular (Fig. 2C, D). To test for immune correlates of hepatic damage, we assessed the cytotoxic granule marker Granzyme B. Interestingly, we observed a strong accumulation of cytotoxic (Granzyme B-positive) CD8 T cells while other Granzyme B-expressing immune cell subsets, such as granulocytes, were not increased (Fig. 2E). These data are also in line with our observation of increased intrahepatic expression of CD38, HLA-DR and transcription factor T-bet as markers of activated effector T cells (Fig. 2A, F). Based on their strong enrichment, widely scattered distribution and activated cytotoxic phenotype within the liver parenchyma, we speculated that CD8 T cells could be drivers of the hepatic inflammation.
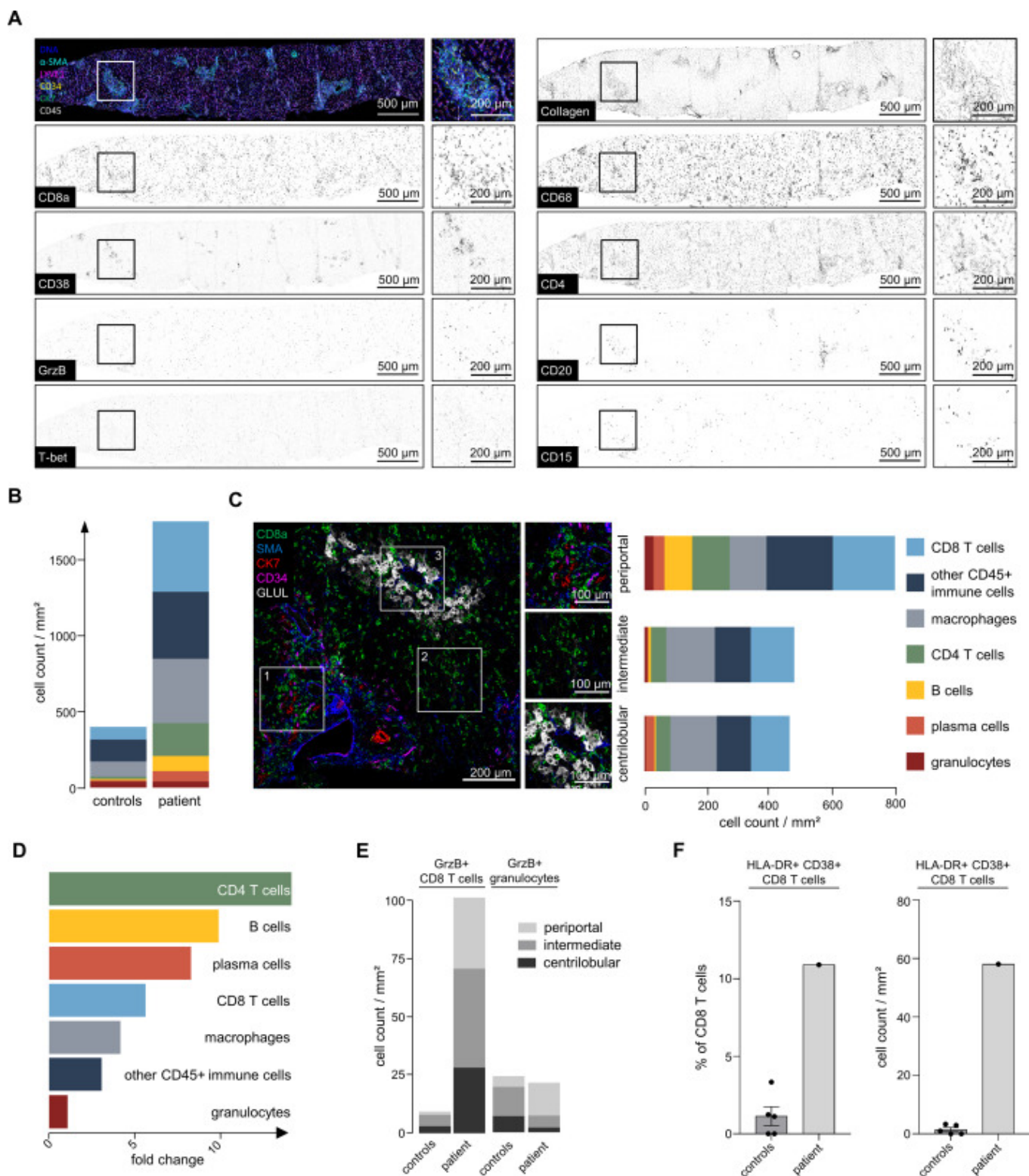
Figure 2. Deep spatial analysis of the hepatic immune environment reveals immune infiltration dominated by cytotoxic CD8 T cells. The liver biopsy was analyzed by highly multiplexed imaging mass cytometry (IMC). A: Pseudocolored IMC images of the liver biopsy. Top left: Composite visualization of CD45, CK7, CD34, LYVE1, a-SMA and DNA are indicated by colors as indicated. Single marker visualization is shown for markers depicted on the left border of the visualizations.

A region of interest is indicated by the box and detailed at higher resolution. Scale bar indicates 500 μm and 100 μm in the inserts respectively. B: Cell counts of immune cell subsets in the liver are shown as stacked barplots compared to controls. C: Composite IMC image visualizing examples of liver zones defined by structural markers: Periportal (top), intermediate (middle) and centrilobular zones (bottom). Immune cell counts within the defined regions visualized as stacked barplots next to the respective inserts. Scale bar indicates 200 μm and 100 μm in the inserts respectively. D: Enrichment of indicated immune populations was calculated by dividing cell density in the patient sample by the mean of control samples. E: Distribution of Granzyme B (GrzB) positive CD8 T cell and granulocyte cell counts within the liver zones. F: Frequency (left) and cell density (right) of HLA-DR+ CD38+ CD8 T cells are shown for the hepatitis patient and controls.

Intrahepatic and longitudinal peripheral immunophenotyping of vaccination-associated CD8 T cell responses

We next performed a detailed analysis of the intrahepatic and peripheral CD8 T cell populations using flow cytometry. The patient's intrahepatic CD8 T cell population was enriched for markers of tissue residency (CXCR6, CD69 and CD103) and activation (CD38) (Fig. 3A). Expression of CD38 on CD8 T cells was also observed in the peripheral blood. Interestingly, CD38 expression levels were markedly elevated in the patient compared to post-vaccination time-point matched control vaccinees that did not develop hepatitis (75.9% vs 15.4%, respectively) (Fig. 3B). The unusual expansion of activated cytotoxic T cells observed in our spatial analysis led us to hypothesize that vaccination-induced SARS-CoV-2 spike-specific CD8 T cells might contribute to liver disease as we have recently observed rapid induction of SARS-CoV-2 spike-specific CD8 T cells by the BNT162b2 mRNA vaccine[15]. Indeed, using a patient-matched HLA-A*03 tetramer loaded with a SARS-CoV-2-spike epitope ($S_{378-386}$) we identified spike-specific CD8 T cells. In the peripheral blood, spike-specific CD8 T cells were 10.2fold more abundant than T cells specific for an EBV-specific CD8+ T cell control epitope (Suppl. Fig. 1). We also identified spike-specific CD8 T cells in the liver. Compared to the peripheral blood, the intrahepatic CD8 T cell pool was ~3.4 fold enriched for spike-specific CD8 T cells (Fig. 3C) and displayed tissue-resident characteristics (CXCR6, CD103, CD69) and strong activation as indicated by CD38 expression (Fig. 3C). Spike protein was not identified in the liver at the time of analysis by immunohistochemistry (data not shown). We next asked whether frequency and activated phenotype of circulating spike-specific CD8 T cells was maintained during therapy. Interestingly, longitudinal analyses showed stable frequencies of circulating spike-specific CD8 T cells (Fig. 3D) with decreasing CD38 expression levels after the initiation of budesonide therapy and coinciding with declining transaminase levels. However, CD38 expression on spike-specific CD8 T cells and other cytotoxicity-associated markers such as GzmB and T-bet increased when the patient relapsed under budesonide therapy, then normalized after introduction of systemic immunosuppressive therapy (Fig. 3E-G). This pattern was not observed for LMP-1$_{419-427}$-loaded HLA-A*24:02-restricted EBV-specific CD8 T

cells (Supp Fig 1). It was also not observed for bulk CD8 T cell analyses, that however showed a high abundance of activated cytototxic CD8 T cell populations in the periphery (Fig. 3E-G). In sum, these data indicate broad activation of cytotoxic CD8 T cells with the peripheral phenotype of spike-specific CD8+ T cells reflecting the clinical response pattern to immunosuppressive therapy.
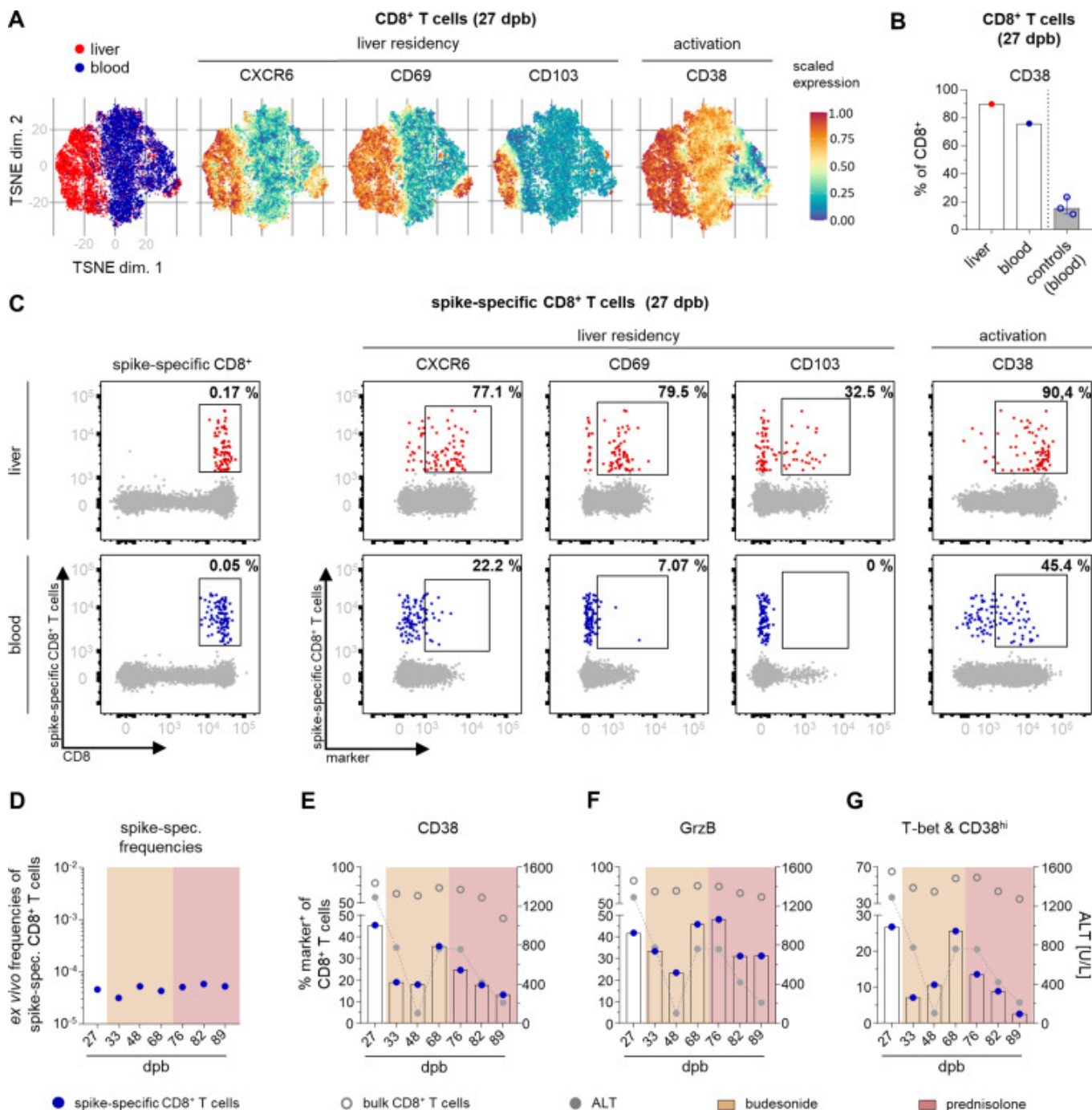
Figure 3. Immunophenotype of peripheral and vaccine-elicited CD8 T cells correlates with hepatitis severity. A: t-SNE representation of flow cytometry data comparing non-naïve CD8+ T

cells 27 days post boost vaccination (dpb) in the patient's liver (red) and blood (blue). Expression levels of CXCR6, CD69, CD103 and CD38 are indicated (blue: low expression; red: high expression). B: Quantified expression levels of CD38, 27 dpb on non-naïve CD8+ T cells within the patient's liver (red) and blood (blue) compared to time-point matched vaccinees without development of hepatitis. C: Original bivariate plots showing frequencies of spike-specific (A*03/S378) CD8+ T cells within the CD8+ T cell population at 27dpb, liver (red) and blood (blue). Expression levels of CXCR6, CD69, CD103 and CD38 of spike-specific CD8+ T cells are indicated. D: Longitudinal analysis of calculated *ex vivo* spike-specific CD8+ T cell frequencies. E: Longitudinal analysis of CD38, F: Granzyme B (GrzB), G: Tbet+CD38hi CD8+ T cells are shown with time-matched ALT (U/l) levels depicted in grey with connected dots, circulating non-naïve spike-specific CD8$^+$ T cells (blue circle) and non-naïve bulk CD8$^+$ T cells (grey open circle). Colored background indicates the patient's therapy regime (orange: budesonide, red: prednisolone).

Discussion

Autoimmune-hepatitis-like disease after vaccination against SARS-CoV-2 is now recognized as a rare adverse event not identified in early trials. The widespread use of the vaccine with administration of hundreds of million doses worldwide raises also questions of causality vs. coincidence. In particular, AIH-like disease after vaccination was reported in patients with age and gender characteristics typical for spontaneous AIH[6, 7, 10]. While some of these cases thus may represent coincidence, a causal relationship to the vaccine is also possible, such as bystander hepatitis driven by elevation of systemic cytokines or chemokines after vaccination, similar to cases occurring in association with natural SARS-CoV-2 infection[13]. The varying patterns of clinical manifestation and the wide range of time elapsed between vaccine administration and symptom onset clearly suggest that different mechanisms may contribute to these reported cases. Here, our analysis highlights that activated cytotoxic CD8 T cells including vaccine-induced spike-specific CD8 T cells could contribute to disease pathogenesis.

Importantly, autoimmune hepatitis is a condition that requires lifelong immunosuppressive therapy in many affected patients[16]. It is therefore important to differentiate AIH from possibly transient immune-mediated hepatitis post vaccination. Diagnosis of autoimmune hepatitis is typically established using AIH scoring tools informed by liver function tests, auto-antibody serology and typical histological features such as interface hepatitis and enrichment of plasma cells[14]. In our case, prior to therapy, AIH diagnosis was deemed "probable" based on the modified original AIH score. It is important to note in this context that the first episode of acute hepatitis after the first vaccine dose was self-limiting without therapy, which also guided our choice to initiate therapy with budesonide in an attempt to minimize systemic side effects and to maintain systemic anti-SARS-Cov2 immunity if possible. However, our patient experienced a relapse 3-4 weeks after budesonide therapy and then required systemic steroid therapy, that was

empirically combined with ursodeoxycholic acid, a combination used in the therapy of autoimmune hepatitis overlap syndrome that was chosen due to presence of AMA-M2 antibodies typically found in primary biliary cholangitis[17]. The patient subsequently recovered quickly, with only a gingivitis occurring during systemic steroid therapy as a possible immunosuppression-related event. Due to relapse hepatitis after steroid tapering, the patient was put under long-term maintenance immunosuppressive therapy under which he achieved complete biochemical remission.

Mechanistically, the disease manifestation in our patient was distinct from classical spontaneous AIH, that is typically associated with elevated peripheral immunoglobulins, a plasma cell dominated infiltrate and prominent interface hepatitis. Here, while there was a slight elevation of peripheral immunoglobulins and intrahepatic enrichment of intrahepatic B cells and plasma cells, a more striking correlate was observed at the level of cytotoxic CD8 T cells. Activated cytotoxic CD8 T cells were strongly enriched in the patient liver to an extent that they represented the most abundant intrahepatic immune cell population and included vaccine elicited SARS-CoV2 specific responses. Notably, the peripheral activation state of these spike-specific CD8 T cells correlated with hepatitis severity and the clinical course after introduction of immunosuppressive therapy. These results implicate T cells as a key pathogenic immune cell type of this vaccine-associated immune hepatitis as a novel subtype of autoimmune hepatitis. The early increase in ALT values after first and second dose of BNT162b2 and the observation that CD8 T cells including spike-specific CD8+ T cells dominate the immune infiltrate also fits to recent observations that demonstrate an early mobilization of spike-specific CD8 T cells already after the first dose of the vaccine [15]. Of note, our tetramer reagent likely stains only a fraction of vaccination-induced antigen-specific T cells, fitting to the broad expression of T cell activation and cytotoxicity markers observed in the analysis of the bulk CD8 T cell population. However, it is also possible that the broad activation pattern observed involves other, non-SARS-CoV2 specific "bystander" CD8 T cell populations. Moreover, the precise mechanism that causes infiltration of the spike-specific CD8 T cells into the liver which adopt features of tissue resident memory T cells (TRM) remains unclear. Virus-specific CD8+ T cells can accumulate in the liver even if the primary site of infection is distant, such as during influenza infection and it is possible that the liver can act as a "graveyard" for activated T cells [18, 19]. However, activated cytotoxic CD8 T cells can mediate hepatitis even in the absence of antigen [20]. In addition, TCR-independent, innate-like cytotoxicity of bystander T cells has been described in acute infections [21, 22]. Of note, CXCR6+ CD8+ TRM cells, such as those found in this patient, may mediate auto-aggression in metabolic liver diseases, in response to local inflammatory cues [23, 24]. Whilst these reports raise the possibility of an antigen-independent T cell-mediated hepatitis, another possible explanation could be the presence of their cognate antigen, i.e. the spike protein. While we could not detect spike protein by IHC in the liver, it has to be noted that biopsy was performed 27 days after the second vaccine dose and transient expression after vaccination, which could have caused CXCR6-expressing spike-specific CD8 T cells to home to the liver and target antigen-presenting cells, cannot be excluded. However, additional mechanisms, such as antigen cross-recognition may

also contribute to the immunopathology. In sum, BNTb163b2 vaccine may trigger immune-mediated hepatitis by mechanisms linked to vaccine-induced cellular immunity. This case illustrates the induction of an unusual CD8 T cell-dominant autoimmune hepatitis after BNT162b2 mRNA vaccination, with enrichment of vaccine-induced SARS-Cov2-specific CD8 T cells. In patients with hepatitis manifesting after the first vaccine dose, additional doses may trigger significant hepatic autoimmunity and require long-term immune suppression.

Methods

Patient samples

A 52-year old male and 3 health care workers (all HLA-A*03:01, confirmed by NGS) >26 days post boost vaccination who received the mRNA vaccine BNT162b2 were recruited at the University Medical Center Freiburg, Germany. Written informed consent was obtained from all participants. Additionally, 5 samples from healthy liver tissue (colorectal cancer liver metastasis-distant tissue) were obtained from the Institute of surgical pathology in Freiburg. The study was conducted according to federal guidelines and local ethics committee regulations (Albert-Ludwigs-University Freiburg, Germany; vote: #21-1135 and #21-1372) and the Declaration of Helsinki (1975).

Imaging mass cytometry

Liver tissue was obtained by transcutaneous biopsy, formalin-fixed, paraffin-embedded, cut into 4 µm sections and stained as previously described.[25] Briefly, after deparaffinization, rehydration, antigen-retrieval and blocking, slides were stained with metal-labeled antibodies and air-dried. Image acquisition of the biopsy (30.912 mm^2) and 2.25 mm^2 of the control samples was performed using a Hyperion Imaging System (Fluidigm; USA). ROIs were laser-ablated spot-by-spot at 200 Hz, resulting in a pixel resolution of 1 µm^2. Image visualization was performed with FIJI (v1.52p, ImageJ). Segmentation of single cells was conducted using an adapted unbiased, supervised analysis pipeline using Ilastik (v 1.3.3) and CellProfiler (v 3.1.9). To analyze liver zones the distance of each pixel to GLUL, CD34 and α-SMA was calculated using CellProfiler (v 4.0.4), added to the high-dimensional information of each cell and used for gating in OMIQ (Omiq Inc). Liver zones were defined: Centrilobular (distance to GLUL ≤50µm), periportal (distance to GLUL >50 µm and distance to CD34 and α-SMA ≤50 µm) and intermediate (distance to GLUL >50 µm and distance to CD34 and α-SMA >50 µm). Absolute cell counts were normalized to 1 mm^2. Stacked barplots were created with R version 4.0.1 using ggplot2.

PBMC isolation

Peripheral blood mononuclear cells (PBMCs) were isolated from anticoagulated blood samples after density gradient centrifugation and subsequently stored at -80°C until further usage.

Single-cell suspension from liver biopsy

Remaining liver tissue was mechanically homogenized and filtered through a 70 µm cell strainer (Corning). Cells were washed and directly processed for flow cytometry analysis. Additionally, freshly isolated PBMCs were also stained and analyzed by flow cytometry.

Analysis of spike-specific CD8+ T cells

SARS-CoV-2 spike peptide ($S_{378-386}$: KCYGVSPTK) was synthesized with a purity of >70% (Genaxxon Bioscience, loaded on HLA-A*03:01 easYmers® (immunAware) and subsequently conjugated with phyocerythrin (PE)-streptavidin (Agilent) according to manufacturer's instructions. Spike(A*03/S_{378})-specific CD8+ T cells were analyzed after magnetic bead-based enrichment as previously described.[10] Briefly, PBMCs were incubated with PE-conjugated tetramerized $S_{378-386}$-loaded HLA-A*03:01 easYmers. Similarly, EBV-specific CD8+ T cells were detected using PE-conjugated tetramerized LMP-1$_{419-427}$-loaded HLA-A*24:02 easYmers. Virus-specific CD8+ T cells were enriched by MACS technology using anti-PE beads. Subsequently, both enriched and pre-enriched samples were analyzed by multiparametric flow cytometry. Frequencies of spike-specific CD8+ T cells were calculated as described before[10,11]. Enriched samples with less than 5 virus-specific CD8+ T cells were excluded from the final analysis, resulting in a detection limit of $5*10^{-6}$ virus-specific CD8+ T cells.

Multiparametric flow cytometry

Antibodies were used for flow cytometry analysis. FoxP3/Transcription Factor Staining Buffer Set (Thermo Fisher) and Fixation/Permeabilization Solution Kit (BD Biosciences) were used for intranuclear and cytoplasmic molecules, respectively. After fixation of cells in 2 % paraformaldehyde/PBS (Sigma), acquisition was performed on LSRFortessa (BD). Data were analyzed with FlowJo, LLC (BD).

Dimensional reduction of multiparametric flow cytometry data

Dimensionality reduction conducted with R version 4.1.1 using Bioconductor (release 3.13) CATALYST (Version 1.16.2). The analyses were performed on live non-naïve CD8+ T cells including the markers CD137, CD39, CD38, CXCR3, CD127, CXCR6, PD-1. Downsampling to 45000 cells was performed. Marker intensities were transformed by arcsinh (inverse hyperbolic sine) with a cofactor of 150. Dimensionality reduction on the transformed data was achieved by t-SNE.

ELISA

Spike-binding antibodies were assessed by Anti-SARS-CoV-2-QuantiVac-ELISA (IgG) (Euroimmun) detecting S1 IgG (<25.6 BAU/ml: negative; 25.6-35.1 BAU/ml: marginally positive; ≥35.2 BAU/ml: positive) according to manufacturer's instructions.

Data availability statement

The generated flow cytometry and imaging mass cytometry datasets will be made available in accordance with legal regulations upon reasonable request.

Funding sources

Conflict of interest statement

The authors declare no conflicts of interest.

Authors contributions:

Study concept and design (TB, MH, BB); experiments and procedures (BC, HS, HL, LW, ESA, KZ, LK, MS); patient sample recruitment (TB, BB), histology assessment (CM,PB), bioinformatics and statistical analysis (BC, HS, HL, ESA); interpretation of data and drafting of the manuscript (TB, MH, BB); revision of the manuscript for important intellectual content (MP, CNH, RT);

Acknowledgments

Appendix A. Supplementary data

The following is/are the supplementary data to this article:

Download : **Download Word document (141KB)**

References

[1]   F.P. Polack, S.J. Thomas, N. Kitchin, J. Absalon, A. Gurtman, S. Lockhart, *et al.*
Safety and Efficacy of the BNT162b2 mRNA Covid-19 Vaccine
New England Journal of Medicine, 383 (2020), pp. 2603-2615
    CrossRef   Google Scholar

[2]   Palla P, Vergadis C, Sakellariou S, Androutsakos T. Letter to the editor: Autoimmune hepatitis after COVID-19 vaccination. A rare adverse effect? Hepatology;n/a.
Google Scholar

[3]   F. Bril, S. Al Diffalha, M. Dean, D.M. Fettig
Autoimmune hepatitis developing after coronavirus disease 2019 (COVID-19) vaccine: Causality or casualty?
Journal of Hepatology, 75 (2021), pp. 222-224
Article   Download PDF   View Record in Scopus   Google Scholar

[4]   D. Clayton-Chubb, D. Schneider, E. Freeman, W. Kemp, S.K. Roberts
Comment to the letter of Bril F et al. "Autoimmune hepatitis developing after coronavirus disease 2019 (COVID-19) vaccine: Causality or casualty?"
Journal of Hepatology (2021)
Google Scholar

[5]   F. Lodato, A. Larocca, A. D'Errico, V. Cennamo
An Anusual Case of Acute Cholestatic Hepatitis After m-RNA BNT162b2 (Comirnaty) SARS-CoV-2 Vaccine: Coincidence, Autoimmunity or Drug Related Liver Injury?
Journal of Hepatology (2021)
Google Scholar

[6]   M.-C. Londoño, J. Gratacós-Ginès, J. Sáez-Peñataro
Another case of autoimmune hepatitis after SARS-CoV-2 vaccination. Still casualty?
Journal of Hepatology (2021)
Google Scholar

[7]   C. McShane, C. Kiat, J. Rigby, Ó. Crosbie
The mRNA COVID-19 vaccine - a rare trigger of Autoimmune Hepatitis?
Journal of Hepatology (2021)
Google Scholar

[8]   A. Rocco, C. Sgamato, D. Compare, G. Nardone
Autoimmune hepatitis following SARS-CoV-2 vaccine: May not be a casuality
Journal of Hepatology (2021)
Google Scholar

[9]   H. Shroff, S.K. Satapathy, J.M. Crawford, N.J. Todd, L.B. VanWagner

Liver injury following SARS-CoV-2 vaccination: a multicenter case series

Journal of Hepatology (2021)

Google Scholar

[10]   C.K. Tan, Y.J. Wong, L.M. Wang, T.L. Ang, R. Kumar

Autoimmune hepatitis following COVID-19 Vaccination: true causality or mere association?

Journal of Hepatology (2021)

Google Scholar

[11]   G.S.Z. Tun, D. Gleeson, A. Dube, A. Al-Joudeh

Immune-mediated hepatitis with the Moderna vaccine, no longer a coincidence but confirmed

Journal of Hepatology (2021)

Google Scholar

[12]   B. Fernando

Autoimmune Hepatitis Developing After Coronavirus Disease 2019 (COVID-19) Vaccine: One or Even Several Swallows Do Not Make a Summer

Journal of Hepatology (2021)

Google Scholar

[13]   G. Kabaçam, S. Wahlin, C. Efe

Autoimmune hepatitis triggered by COVID-19: A report of two cases

Liver International, 41 (2021), pp. 2527-2528

CrossRef   View Record in Scopus   Google Scholar

[14]   F. Alvarez, P.A. Berg, F.B. Bianchi, L. Bianchi, A.K. Burroughs, E.L. Cancado, *et al.*

International Autoimmune Hepatitis Group Report: review of criteria for diagnosis of autoimmune hepatitis

Journal of Hepatology, 31 (1999), pp. 929-938

Article   Download PDF   CrossRef   View Record in Scopus   Google Scholar

[15]   V. Oberhardt, H. Luxenburger, J. Kemming, I. Schulien, K. Ciminski, S. Giese, *et al.*

Rapid and stable mobilization of CD8+ T cells by SARS-CoV-2 mRNA vaccine

Nature (2021)

Google Scholar

[16]   EASL Clinical Practice Guidelines

Autoimmune hepatitis

Journal of Hepatology, 63 (2015), pp. 971-1004

Google Scholar

[17] Z.M. Younossi, D. Bernstein, M.L. Shiffman, P. Kwo, W.R. Kim, K.V. Kowdley, *et al.*
Diagnosis and Management of Primary Biliary Cholangitis
The American journal of gastroenterology, 114 (2019), pp. 48-63
CrossRef   View Record in Scopus   Google Scholar

[18] W.Z. Mehal, A.E. Juedes, I.N. Crispe
Selective retention of activated CD8+ T cells by the normal liver
J Immunol, 163 (1999), pp. 3202-3210
View Record in Scopus   Google Scholar

[19] G.T. Belz, J.D. Altman, P.C. Doherty
Characteristics of virus-specific CD8(+) T cells in the liver during the control and resolution phases of influenza pneumonia
Proc Natl Acad Sci U S A, 95 (1998), pp. 13812-13817
View Record in Scopus   Google Scholar

[20] D.G. Bowen, A. Warren, T. Davis, M.W. Hoffmann, G.W. McCaughan, B. Fazekas de St Groth, *et al.*
Cytokine-dependent bystander hepatitis due to intrahepatic murine CD8 T-cell activation by bone marrow-derived cells
Gastroenterology, 123 (2002), pp. 1252-1264
Article   Download PDF   View Record in Scopus   Google Scholar

[21] J. Kim, D.Y. Chang, H.W. Lee, H. Lee, J.H. Kim, P.S. Sung, *et al.*
Innate-like Cytotoxic Function of Bystander-Activated CD8(+) T Cells Is Associated with Liver Injury in Acute Hepatitis A
Immunity, 48 (2018), pp. 161-173
e165
Google Scholar

[22] E. Sandalova, D. Laccabue, C. Boni, A.T. Tan, K. Fink, E.E. Ooi, *et al.*
Contribution of herpesvirus specific CD8 T cells to anti-viral T cell response in humans
PLoS Pathog, 6 (2010), Article e1001051
CrossRef   Google Scholar

[23] M. Dudek, D. Pfister, S. Donakonda, P. Filpe, A. Schneider, M. Laschinger, *et al.*
Auto-aggressive CXCR6(+) CD8 T cells cause liver immune pathology in NASH
Nature, 592 (2021), pp. 444-449
CrossRef   View Record in Scopus   Google Scholar

[24] D. Pfister, N.G. Nunez, R. Pinyol, O. Govaere, M. Pinter, M. Szydlowska, *et al.*
NASH limits anti-tumour surveillance in immunotherapy-treated HCC
Nature, 592 (2021), pp. 450-456

CrossRef   View Record in Scopus   Google Scholar

[25]   M. Schwabenland, H. Salié, J. Tanevski, S. Killmer, M.S. Lago, A.E. Schlaak, *et al.*
       Deep spatial profiling of human COVID-19 brains reveals neuroinflammation with distinct microanatomical microglia-T-cell interactions
       Immunity, 54 (2021), pp. 1594-1610
       e1511
       View Record in Scopus   Google Scholar

Cited by (0)

*   equal contribution

View Abstract